MICROFLUIDICS IN THE UNDERGRADUATE LABORATORY:

Device Fabrication and an Experiment to Mimic Intravascular Gas Embolism

ERIN L. JABLONSKI, BRANDON M. VOGEL, DANIEL P. CAVANAGH
Bucknell University • Lewisburg, PA, 17837
KATHRYN L. BEERS
National Institute of Standards and Technology • Gaithersburg, MD, 20879

Microfluidic technology is rapidly finding utility in a wide range of applications from chemical synthesis and separations to genetics and biochemical assays.[1,2] The flow of nanoliter quantities of fluids through micrometer-scale channels offers a unique environment for improved flow control, heat transfer, and fluid mixing.[3] The prohibitive expense of manufacturing microfluidic devices, however, has created a significant barrier to the use of microfluidics for academic instruction. Traditional manufacturing methods involve aggressive chemical etching or sensitive photolithographic techniques that require clean room facilities. Some fabrication techniques lessen the need for these clean room facilities, but still require fabricating an expensive negative master to reproduce channels in an elastomeric material.[4] Having a safe, inexpensive, and versatile method to prepare masters for microfluidic devices in a typical lab environment[5,6] creates an opportunity to develop laboratory experiments that reinforce basic ideas in subjects from chemistry and biology to chemical engineering and materials science. Besides bubble-flow analysis, microfluidic devices can be used to study myriad fluid dynamics phenomena in different channel geometries.

The experiment detailed here involves the break-up of air bubbles in an aqueous flow. Droplet and bubble break-up have been studied extensively in the literature experimentally and numerous models have been proposed that describe droplet break-up in microchannels. An excellent review of droplet dynamics is provided by Cristini and Tan.[7] Jousse, *et al.*, provide an analysis of both experimental and theoretical work involving the dynamics of the flow of droplets.[8] Specifically, they characterize the flow of droplets from a single parent channel into two daughter channels. Leshansky and Pismen detail the behavior of droplets incident on a T-junction and

Erin L. Jablonski *is an assistant professor in the Department of Chemical Engineering at Bucknell University. Her interests in engineering education include effective integration of classroom and laboratory activities through project-based design. Her research interests are in the characterization of surface chemical properties and diffusion in polymeric materials.*

Brandon M. Vogel *is an assistant professor of chemical engineering and is a Jane W. Griffith Fellow at Bucknell University. He received his B.S. in chemistry and B.ChE. from the University of Minnesota, Twin Cities, and his M.S. and Ph.D. in chemical engineering from Iowa State University. He teaches biomaterials, bioprocess engineering, senior design, and statistics. His research interests include the synthesis of new materials to detect, target, and treat disease.*

Daniel P. Cavanagh *is chair and associate professor in the Department of Biomedical Engineering at Bucknell University. He currently holds the Richard C. and Gertrude B. Emmitt Memorial Chair in Biomedical Engineering and was awarded the Christian R. and Mary F. Lindback Award for Distinguished Teaching at Bucknell University. His research interests focus on the use of microfluidic technology to investigate the mechanics of intravascular gas embolism.*

Kathryn L. Beers *is the deputy division chief and Sustainable Polymers Group leader in the Polymers Division of the National Institute of Standards and Technology. Her current interests include the use of microfluidics and microreactors for polymerizations based on renewable feedstocks and using green transformation routes. In the past, her research focused on measurements of polymers at interfaces, and polymerizations in confined spaces, as well as developing microfluidic technology for complex fluid measurements.*

describe the contribution of the capillary instability to droplet break-up in their system.[9] Droplet traffic at a T-junction has been well characterized by Engl, *et al.*, who present a method to determine how the "feedback" from droplets beyond a junction point influences the behavior of subsequent droplets upstream.[10] Several researchers have investigated droplet break-up at junctions of arbitrary angle, both experimentally and theoretically, for a broad range of flow conditions.[11,12]

OVERVIEW OF THE EXPERIMENT

This experiment introduces students to the design and fabrication of a microfluidic device. In fabricating the device, students use processing steps common to lithography; a photomask and ultraviolet (UV) exposure source are used to pattern a negative-tone photoresist and contact lithography is then performed using a mold. The strengths of the device-fabrication method are ease and low cost of producing masters that are traditionally difficult and prohibitively expensive to make.

The flow experiment presented allows students to investigate the behavior of bubbles in liquid flows as a model of intravascular gas embolism, or the presence of gas bubbles in the bloodstream. The microfluidic environment facilitates the investigation of bubble dynamics as a function of bubble size and bulk liquid flow rate at biologically relevant length scales. Through using microbubbles to model the behavior of gas emboli in the small model vasculature, students gain an appreciation of the dynamics of fluid behavior at smaller scales. Without prior preparation by a laboratory instructor, designing and fabricating the microfluidic device requires three successive laboratory sessions. The laboratory instructor, however, can reduce this to one meeting with sufficient preparation—particularly of the release and frame layers. To expedite the process, the instructor can prepare master slides that students can use to pattern polydimethylsiloxane (PDMS), and have patterned PDMS ready to be sealed against glass, so that students will carry out all aspects of the fabrication but not have to wait for PDMS to degas or cure before moving on to the next step. For the experiment modeling gas bubbles in the bloodstream, one laboratory session should be enough to observe bubble dynamics with varying flow conditions.

MATERIALS AND EQUIPMENT†

I. Device Fabrication

After mask design, the microfluidic device is created by preparing a negative of the channel in a thiolene-based resin using masks such as those in Figure 1. The negative is then reproduced in PDMS and sealed against a glass slide. Small-gauge Teflon (or Stainless steel) tubing is inserted into the PDMS at the circular channel ends for inlets and outlets. Equipment necessary for the fabrication procedure includes a radio frequency (RF) plasma etcher (with oxygen or air) (REFLEX Analytical Corporation) and an ultraviolet (UV) flood exposure source (365 nm, UVA) (Spectronics).

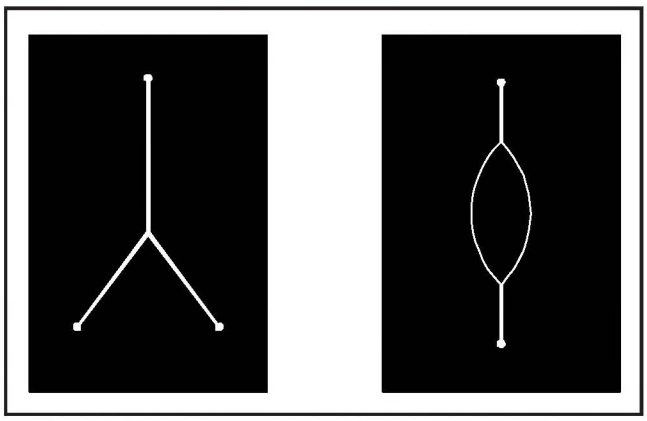

Figure 1. *Typical photomasks used for microfluidic device masters.*

The materials needed for device fabrication include glass slides (2 in. × 3 in.), a polystyrene container (15 cm × 20 cm × 2 cm) (or large glass Petri dish 20 cm diameter), thiolene optical adhesive (NOA-81 resin, Norland Products Inc., Cranbury, NJ), and PDMS prepolymer (Sylgard 184, Dow-Corning).

The microfluidic mask can be designed using a software package such as Microsoft Publisher, Canvas, or Adobe Illustrator.

The PDMS release (for fabricating the master mold) and frame (supports the mold during device fabrication) layers were prepared in advance. Aluminum foil was used to protect the benchtop and to prevent spreading the PDMS solution to surrounding areas in the laboratory. From the Sylgard 184 kit, the silicone elastomer base and curing agent were mixed in a 10:1 ratio in a disposable beaker. This PDMS solution was vigorously mixed with a disposable utensil for approximately 3-5 min or until the solution was opaque with bubbles. For the release layer, the PDMS solution was poured into a container approximately 15 cm × 20 cm × 2 cm (or into a glass Petri dish with 20 cm diameter). The release layer stays in its container and can be used multiple times; it is convenient to have several release layers for quickly fabricating multiple devices. For the frame, the PDMS solution was poured into a 10 cm × 15 cm × 0.5 cm polystyrene container. The frame is removed from its container, so this container is disposable. The PDMS solution was de-gassed in a vacuum desiccator by pressurizing and depressurizing the unit until all the bubbles were removed. This process takes about one hour, depending on the quantity of PDMS solution. When the PDMS solution was devoid of bubbles, the containers were placed into an oven for at least 3 hr at 70 °C. The oven shelf must be level to ensure even curing of the release layer and frame.

† *Equipment and instruments or materials are identified in the paper in order to adequately specify the experimental details. Such identification does not imply endorsement by the authors, nor does it imply the materials are necessarily the best available for the purpose.*

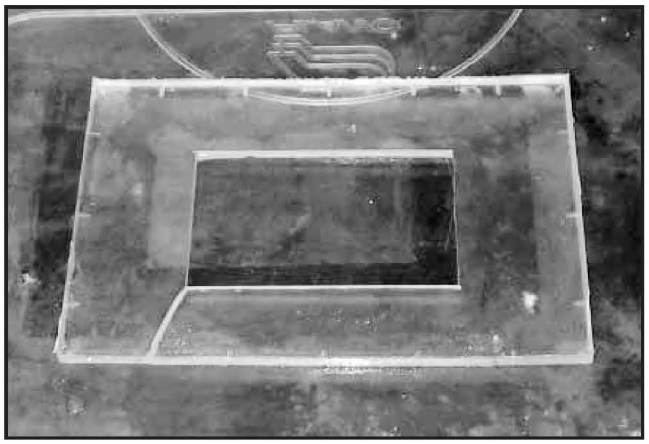

Figure 2. *PDMS frame layer on top of a PDMS release layer.*

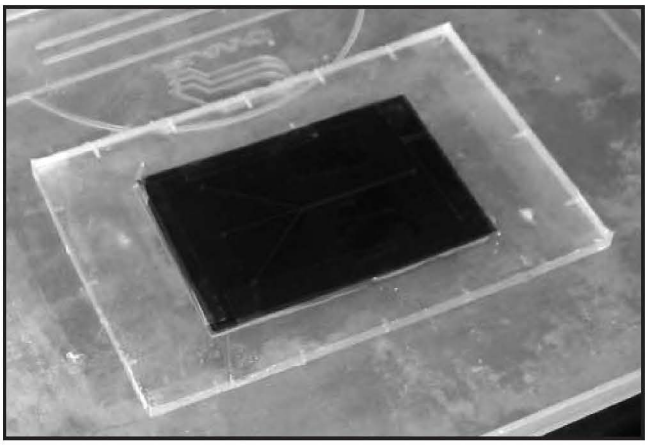

Figure 3. *Mask added to glass slide on top of the PDMS frame containing optical adhesive.*

The frame slab was carefully removed from the polystyrene container and a razor blade was used to cut a rectangular hole in the center of the slab. The inner dimensions of the frame are slightly smaller than the glass slide used to create the microfluidic device. The frame was placed in the center of the release layer, as shown in Figure 2.

Photomasks were created with the desired device designs using Microsoft Publisher and printed on a transparency with a 1200-dpi (or better) resolution laser printer (HP 8000). The photomask may contain any pattern provided the dimensions are suitable for the glass slide. The optical adhesive used to make the master is a negative-tone photoresist. Therefore, the mask background is black, while the lines that will become the microfluidic channels are white, as shown in Figure 1. UV light polymerizes optical adhesive in only the white part of the mask. In the photomask, small circles were added to the end of the lines where the entry and exit points are located to facilitate connecting the channels to the syringe pumps (optional). To ensure complete opacity of the photomask, two copies of the photomask were printed on a transparency and then taped with the channels of both copies carefully aligned.

To make the master (the mold used to imprint a PDMS slab to make the microfluidic device), a commercially available optical adhesive, NOA-81, was used. NOA-81 is stored in the refrigerator and must be allowed to come to room temperature before use. The glass slide that became the substrate for the master was cleaned with absolute ethanol and dried with compressed air, then placed in the RF plasma cleaner (oxygen or air plasma) for 5 min at full power. To fabricate the master, the NOA-81 solution was poured into the frame on the release layer until the frame was filled and nearly overflowing. Any air bubbles were allowed to dissipate or were carefully popped with a razor blade. The plasma-cleaned glass slide was allowed to cool in the plasma cleaner for a few minutes, and then carefully laid over the NOA-81 to avoid trapping any air bubbles underneath the slide. The photomask was positioned on top of the glass slide, as shown in Figure 3. This assembly was placed under a flood UV source roughly 15 cm from the light source and cured for 3 min to 5 min. Getting the appropriate feature height requires some trial and error to optimize the exposure time and distance from the UV lamp. The resulting feature height was measured with a micrometer.

After the UV exposure, the photomask was lifted off and the glass slide (master) was carefully removed from the frame. The master has raised crosslinked areas where the photomask is transparent and uncrosslinked adhesive on other portions. Using compressed air (house line is suitable), as much of the uncured adhesive as possible was blown away. The master was washed with absolute ethanol to remove more of the uncured adhesive. A razor blade was used to remove any excess unreacted material from the edges. The master was then carefully washed with a small volume (10 mL) of acetone and then immediately washed again with copious amounts of absolute ethanol. Acetone can cause delamination if left on the master for too long. It is important to remove the excess adhesive to create a device with features that replicate the photomask pattern. After removing the excess adhesive, the master was subjected to a second UV exposure (post-cure) (with lamp ≈15 cm away) for approximately 20 min. The master was then baked at 50 °C in an oven overnight to adhere the NOA-81 to the glass slide (Figure 4, next page). A master that is properly cleaned and fully cured will last for many PDMS reproductions.

The master was used to mold a slab of PDMS by placing the master with the raised mold facing up into an appropriately sized "boat" made from aluminum foil. The "boat" was then filled with PDMS solution and the PDMS was cured in the oven.

The patterned PDMS slab still on the master was removed gently from the foil and a razor blade was used to trim the excess PDMS that exceeded the dimensions of the glass slide. The patterned PDMS slab was then carefully peeled away

from the master. It is important the patterned PDMS slab not be cracked when being removed from the master. A needle (or punch) was used to puncture holes through the PDMS where the circular entry ports were patterned. A new glass slide that had been cleaned with ethanol and dried with compressed air and the patterned PDMS slab (pattern side up) were placed into the oxygen plasma cleaner for five minutes on the lowest setting. (Determination of the suitable time/power of plasma exposure for proper device sealing may require trial and error.*) After plasma cleaning, the glass slide and patterned PDMS slab were pressed together to form the microfluidic device. To improve bonding between the PDMS slab and glass slide, they were placed in an oven at 70 °C for about 10 min. Hollow metal or flexible capillary Teflon tubing was inserted to create ports of entry and exit. Figure 5 is an image of the completed device.

II. Gas Emboli in Model Blood Flow Experiment

The major components of the experimental setup are: two multisyringe infusion/withdrawal syringe pumps (one for bulk fluid, one for air infusion) (Cole-Parmer), binocular low-power compound microscope with high-speed digital camera linked to computer with image processing software (Cole-Parmer), a high-speed imaging system (Roper Scientific, Motion Corder SR-500), and the microfluidic device.

In preparation for running the gas emboli experiment, a 60 mL syringe was loaded with approximately 50 mL of water. Next, a 20 mL syringe was filled with air. A 60 cm piece of luer-lock tubing was used to connect the 60 mL syringe to one port on the three-way luer-lock stopcock. Using a second 60 cm piece of luer-lock tubing, the 20 mL syringe was connected to an open port on the stopcock. A third piece of luer-lock tubing was used to connect the outflow port of the stopcock to the inlet channel on the microfluidic device. The stopcock was set to have all three pathways open.

With the microfluidic device securely placed on the stage of the microscope, the device was aligned on the stage for optimal viewing of both the parent tube and the bifurcation point. An image acquisition rate of 500 frames/s (fps) was used.† The bulk liquid syringe pump was set at a flow rate less than or equal to 3 mL/min. The flow was maintained long enough to flush any residual air from the liquid flow tubes and the microfluidic device. Once the liquid path was clear of bubbles, the air syringe pump was started at a flow rate less than that of the liquid pump. In general, if the bubbles in the system are very long or are passing the bifurcation at a very high frequency, the flow rate may be decreased to produce smaller and fewer bubbles. Several air bubbles were allowed to traverse the microfluidic device to verify the correct operation of the system. On verification of correct operation, the air syringe pump was turned off and the liquid pumping was used to flush any remaining air from the system. The liquid pump was then turned off in preparation for starting the experiment.

For the experimental microfluidic device described here,

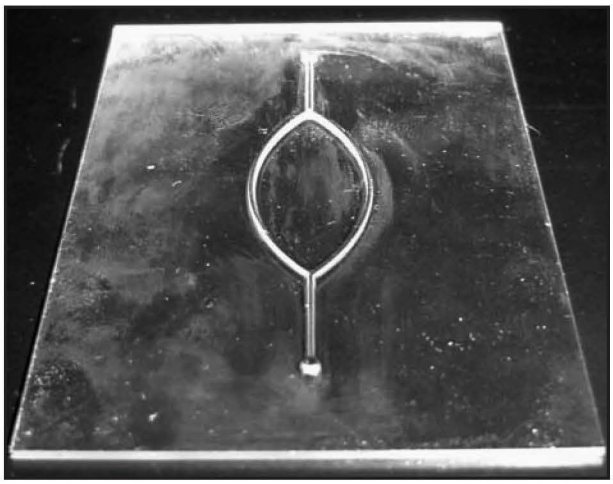

Figure 4. *(above) Completed master of optical adhesive on glass.*

Figure 5. *(below) Completed microfluidic devices showing inlet and outlet ports using hollow metal tubing ports and large flexible tubing connectors.*

* *If a radio frequency plasma cleaner is unavailable, an alternative and less expensive method for bonding PDMS to glass is detailed in Reference 13.*

† *The necessary camera speed (fps) for capturing bubble bifurcation is dependent on the velocity through the channels. Depending on the camera available, the flow rates should be adjusted accordingly.*

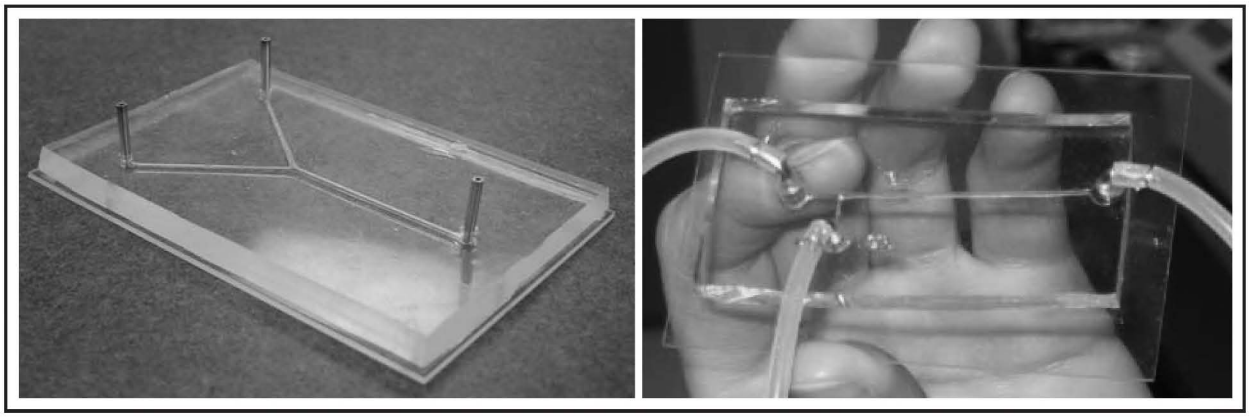

the parent channel dimensions are 280 μm high and approximately 500 μm wide, splitting into two daughter channels each having a width of nearly 250 μm. The cross-section of the channels has a semicircular shape. The dimensions of the photomask control the channel widths but the UV exposure time fixes the channel height (longer exposure times give taller features but compromise lateral resolution). These channel sizes approximate the size of an artery or vein and are easy to obtain with a photomask printed on a laser jet printer with a minimum resolution of 1200 dots per square inch (dpi).

EXPERIMENTAL METHODS AND RESULTS

The bulk fluid syringe pump infuses the bulk liquid (water or blood mimic) through 1.59 mm ID luer tubing to a three-way stopcock. A second syringe pump infuses air into another port on the stopcock. Bubble-laden flow exits from the stopcock by 1.59 mm ID tubing that is attached to the port inserted in the microfluidic device at the entrance to the parent channel. The behavior of the bubbles as they traverse the bifurcation is recorded with the digital imaging system. After flowing through the device, the fluid with bubbles leaves through exit ports into a waste container. The bulk liquid syringe pump flow rate is varied between 2.0 and 3.0 mL/min as this range is representative of flows found in similarly sized blood vessels (Table 1). The bulk flow rate of 3 mL/min was found to be the highest flow rate allowable to still record quality images with the digital imaging system at its maximum rate of 500 fps. While it is possible to obtain images at a rate as low as 100 fps, it is difficult to observe bubble-splitting behavior at this rate. The experimental bubbles were infused into the bulk flow by the second syringe pump that was set at a flow rate lower than the bulk flow syringe pump. Because of the dynamic nature of bubble formation upon infusion into the bulk flow, creating successive bubbles of identical size was difficult. Therefore, the typical approach used in these experiments was to record 8-10 seconds of images that were later examined using image processing software‡ to measure and group bubbles by size.

To perform the required image analysis, images recorded by the camera mounted on the microscope were downloaded to a computer. Besides permitting the transfer of images to the computer, this imaging setup also enables the user to view the same images through the optical lens of the microscope during the experiments. To test the repeatability of the experiments, each combination of bubble size and bulk liquid flow rate was carried out four times.

TABLE 1
Properties of Blood Flow in Vessels. Reynolds number values calculated for blood flows in blood vessels. The standard uncertainty of the measured values is ± 5%.

Vessel	Inner Diameter (mm)	Velocity (cm/s)	Re
Arteries	0.15 to 15	10 to 40	500
Arterioles	0.01 to 0.14	0.1 to10	0.7
Capillaries	0.008	< 0.1	0.002
Venules	0.01 to 0.14	< 0.3	0.01
Veins	0.15 to15	0.3 to 5	150

With the system primed and flushed of air as instructed above, the image acquisition system was activated to record continuously and store 8 seconds of images. The bulk liquid syringe pump was started and liquid pumping continued until there were no bubbles in the flow path. With a clear flow path and readied image acquisition system, the air syringe pump was started to infuse air into the flow path. In general, it may be necessary to adjust the flow rate of air to produce a steady stream of bubbles with the desired size. With a stream of bubbles flowing through the microfluidic device, the image acquisition system was started to record 8-10 seconds of images at 500 fps.

The image files were examined to find sequences of images that contain bubbles traversing the bifurcation. The axial length of the bubble in the parent tube was measured to classify the bubbles-size categories. The behavior of the bubble was then examined as it traversed the bifurcation to further classify bubbles based upon behavior at the branching point. Bubbles are grouped by size and behavior to examine the correlation between the two. To examine the effects of bulk liquid flow rate, this experimental process can easily be repeated for different bulk liquid flow rates. After running a series of experiments examining various bubble sizes and flow rates, the user can create a table that indicates the observed behavior of bubbles of specific sizes at specific flow rates. This table can be used to determine the effect of bulk liquid flow rate and bubble size on bubble behaviors at bifurcations in channels of known size.

Upon completing the investigation, many possibilities exist for extending the experiments for further investigations. These additional possibilities may also be used by an instructor to provide for experimental variations between laboratory groups. Possible modifications include varying the bulk fluid including water, oil, or xantham gum solutions as blood analogs. An independent experiment to determine the viscosity of the bulk fluid should be carried out. Different microfluidic device designs can also be used. Finally, two immiscible liquids could be used to examine liquid droplet behavior in surrounding liquid streams. In general, this experiment provides for a wide range of experimental possibilities.

DISCUSSION

The relevant parameters that best characterize the behavior of liquid flows in pipes or channels are average velocity and Reynolds number (Re). The average velocity and Re of actual

‡ *The authors recommend ImageJ (Reference 15). Matlab can also be used for image analysis.*

blood flow in blood vessels are dependent on the diameter of the vessel as shown in Table 1 where representative values are listed.[14] These values are calculated using the definition of Re for flow in circular pipes, $Re = \rho VD/\mu$, where D is pipe diameter, ρ is the density of the fluid [g/cm^3], V is the average fluid velocity [cm/s], and μ is the fluid viscosity [g/cm·s]. Because one of the goals of this experiment is for students to characterize the fluid flow by calculating Re, the noncircular cross-sectional profile of the channels must be considered. This is accomplished by replacing the pipe diameter, D, in the equation above with the hydraulic diameter (D_H) resulting in the following equation, $Re = \rho VD_H/\mu$, with $D_H = 4A/P_W$ where A and P_W are the cross-sectional area and wetted perimeter of the channel, respectively. Therefore, Re of the fluid flows in the parent channels in this experiment can be calculated given $\rho_{water} = 1.0$ g/mL and $\mu_{water} = 0.01$ cP. For flow rates ranging from 2 mL/min to 3 mL/min, the Reynolds number is $30 < Re < 50$. Assuming the definition of laminar flow in a circular pipe ($Re < 2000$) can be applied to this semi-circular channel system, the flows in this experiment are laminar.

Bubbles introduced into the fluid flow move with the fluid because of the pressure gradient produced within the channel by the syringe pump. When a bubble meets a division (Figure 6a, 6b), the leading edge of the bubble stops at the apex and the trailing edge continues to move. If the trailing liquid-gas boundary has enough momentum to reach the junction, a pinch point forms and the bubble splits (Figure 6c and 6d). Conversely, if the trailing liquid-gas boundary does not have enough momentum, the bubble does not break but instead flows to one side of the division.

The observed behaviors of bubbles traversing the bifurcation as a function of bubble size and flow rate are presented in

TABLE 2

Behavior of bubbles traversing bifurcations as a function of Reynolds number (Re) and bubble size (λ). A = no bubble division; B = bubble division; L and R indicate into which channel bubbles traveled; B* = bubble division with daughter bubble lodged in daughter channel.

	Reynolds number (Re) in the parent channel		
Re/λ	33	41	50
1.5 – 1.99	A (2L:2R)	A (4L)	A (4L)
2.0 – 2.49	A (3L;1R)	A (2L:2R)	A (4L)
2.5 – 2.99	B*	B*	B
3.0 – 3.49	B	B	B
3.5+	B	B	B

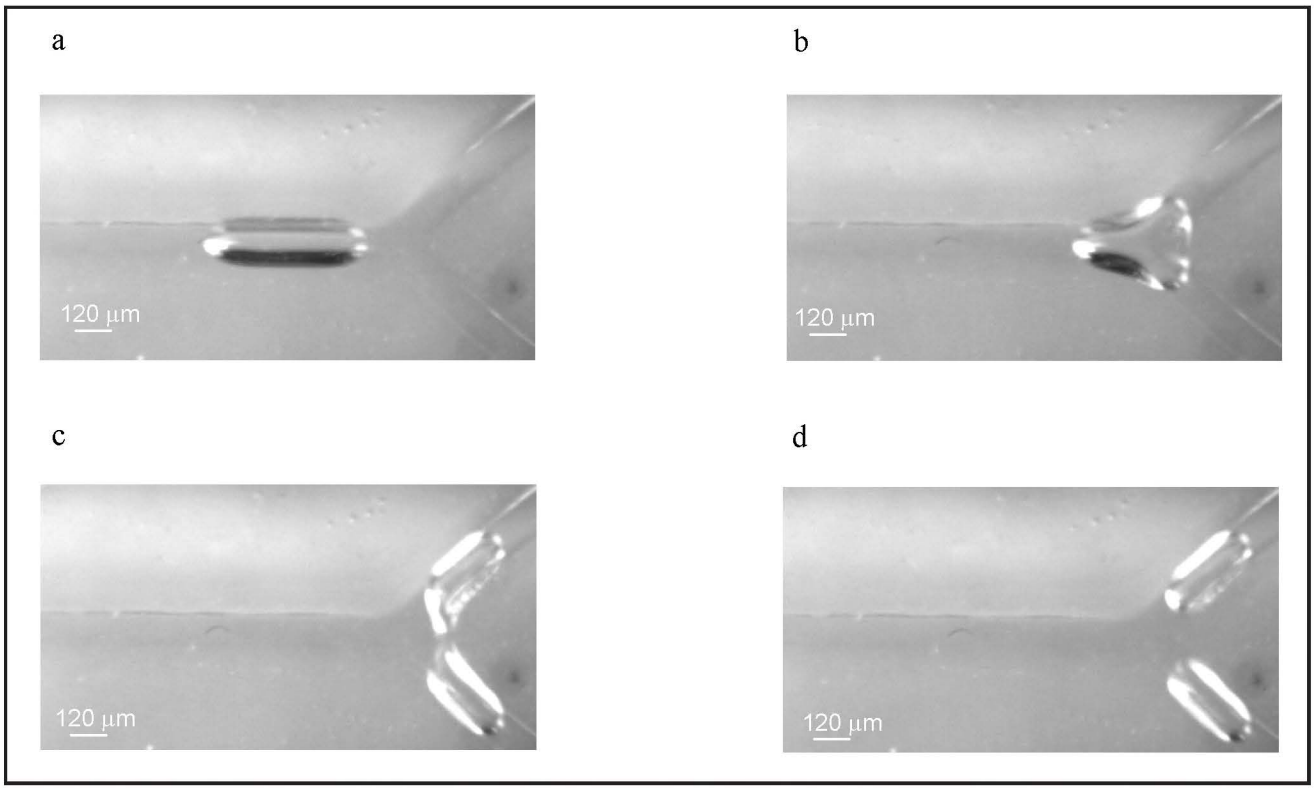

Figure 6. *Images of bubble (the dark shape) flow behavior at a bifurcation in a microfluidic device. a) The leading edge of the bubble hits the bifurcation. b) The bubble splits as the trailing edge flows toward the bifurcation. c) The trailing edge of the bubble hits the bifurcation. d) The bubble splits into two separate bubbles as they continue to flow down the daughter channels of the device.*

Table 2. In general, two distinct behaviors are found. The first, indicated as type A, is when the entire bubble travels down either the left (L) or right (R) daughter tube without dividing. With each type A behavior in Table 2, we also indicate into which daughter channel (L or R) each of the bubbles traveled in the four experimental trials. The second type, indicated as type B, occurs when the bubble divides at the bifurcation producing a daughter bubble in each daughter channel. Also, for two combinations of Re and λ, we observed a few instances where after dividing, one of the daughter bubbles became lodged in a daughter channel. These behaviors are indicated as B*.

Overall, bubbles are more likely to break if they are relatively large for the characteristic length of the channel and are in a liquid flow with a higher Re. Larger bubbles have a "sausage" shape in the channel; they form this shape to lower the interfacial surface area between the gas and the fluid. The small size of the channel inhibits the bubbles from forming a perfect sphere (the lowest free-energy shape). Because the "sausage" shape is not the preferred shape for the bubble, it is unstable and will break at the division to lower its energy (interfacial surface area) if given enough momentum. Alternatively, a bubble may remain intact if there is not enough momentum to destabilize it at the division or if one daughter channel offers lower resistance to flow (that is, is larger than the other daughter channel). The bubbles that are smaller than the width of the channel are able to preserve their lowest energy shape (the sphere) and therefore they do not need to break at the apex to lower their energy. Students can experimentally discover many of these phenomena using devices with several different channel configurations. It is important to point out that observations from this simple microbubble experiment may give insight to potential paths to reduce emboli.

CONCLUSION

We present a protocol for fabricating microfluidic devices and results from an example experiment modeling intravascular gas emboli that occur in the bloodstream. Microfluidic devices are well suited for this investigation because they contain channels with cross-sectional dimensions in the ~500 μm range depending on the fabrication procedure. The advantages to these devices are their low cost, small sample size, and quick analysis. The designs of the channels are limitless and allow for a wide range of experiments including mixing chemical solutions, filtering of solutions, liquid chromatography and microchemical reactors. With this fabrication protocol, undergraduate students will be able to perform laboratory exercises involving microfluidic technology.

ACKNOWLEDGMENTS

The authors thank Kristin McDonnell, Tracey Perry, Lisa Schultz, Lauren Shafer, and Amy Ukena (Bucknell University) for their work on the experimental protocol.

REFERENCES

1. Auroux, P.A., D. Iossifidis, D.R. Reyes, and A. Manz, "Micro Total Analysis Systems 2. Analytical Standard Operations and Applications," *Analytical Chemistry*, **74**(12), 2637 (2002)
2. Vilkner, T., D. Janasek, A. Manz, "Micro Total Analysis Systems. Recent Developments," *Analytical Chemistry*, **76**(12), 3373 (2004)
3. Reyes, D.R., D. Iossifidis, P.A. Auroux, and A. Manz, "Micro Total Analysis Systems 1. Introduction, Theory, and Technology," *Analytical Chemistry*, **74**(12), 2623 (2002)
4. Xia, Y.N., and G.M. Whitesides, "Soft Lithography," *Angewandte Chemie-International Edition*, **37**(5), 551 (1998)
5. Cabral, J.T., S.D. Hudson, C. Harrison, and J.F. Douglas, "Frontal Polymerization for Microfluidic Applications," *Langmuir*, **20**(23), 10020 (2004)
6. Harrison, C., J. Cabral, C.M. Stafford, A. Karim, and E.J. Amis, "A Rapid Prototyping Technique for the Fabrication of Solvent-Resistant Structures," *J. Micromechanics and Microengineering*, **14**(1), 153 (2004)
7. Cristini, V., and Y.-C. Tan, "Theory and Numerical Simulation of Droplet Dynamics in Complex Flows—a Review," *Lab on a Chip*, **4**(4), 257 (2004)
8. Jousse, F., R. Farr, D.R. Link, M.J. Fuerstman, and P. Garstecki, "Bifurcation of Droplet Flows within Capillaries," *Physical Review E*, **74**(3), 036311-1 (2006)
9. Leshansky, A.M., and L.M. Pismen, "Breakup of Drops in a Microfluidic T Junction," *Physics of Fluids*, **21**(2), 023303-1 (2009)
10. Engl, W., M. Roche, A. Colin, and P. Panizza, "Droplet Traffic at a Simple Junction at Low Capillary Numbers," *Physical Review Letters*, **95**(20), 208304-1 (2005)
11. Menetrier-Deremble, L., and P. Tabeling, "Droplet Breakup in Microfluidic Junctions of Arbitrary Angles," *Physical Review E*, **74**(3), 035303-1 (2006)
12. Link, D.R., S.L. Anna, D.A. Weitz, and H.A. Stone, "Geometrically Mediated Breakup of Drops in Microfluidic Devices," *Physical Review Letters*, **92**(5), 054503-1 (2004)
13. Haubert, K., T. Drier, D. Beebe, "PDMS Bonding by means of a Portable, Low-cost Corona System," *Lab on a Chip*, **6**(12), 1548 (2006)
14. Muth, C.M., and E.S. Shank, "Gas Embolism," *New England Journal of Medicine*, **342**(7), 476 (2000)
15. Collins, T.J., "ImageJ for Microscopy," *BioTechniques*, **43**(1), S25 (2007) ❐